Letter

The Sun as a target for axion dark matter detection

Elisa Todarello [a,b], [*], Marco Regis [a,b],[*], Marco Taoso [b], Maurizio Giannotti [c], Jaime Ruz [c], Julia K. Vogel [c]

[a] *Dipartimento di Fisica, Università di Torino, Via P. Giuria 1, 10125 Torino, Italy*
[b] *Istituto Nazionale di Fisica Nucleare, Sezione di Torino, Via P. Giuria 1, 10125 Torino, Italy*
[c] *Centro de Astropartículas y Física de Altas Energías (CAPA), Universidad de Zaragoza, Zaragoza, 50009, Spain*

ARTICLE INFO

Editor: A. Ringwald

ABSTRACT

The exploration of the parameter space of axion and axion-like particle dark matter is a major aim of the future program of astroparticle physics investigations. In this context, we present a possible strategy that focuses on detecting radio emissions arising from the conversion of dark matter axions in the Sun's magnetic field, including conversion in sunspots. We demonstrate that near-future low-frequency radio telescopes, such as the SKA Low, may access regions of unexplored parameter space for masses $m_a \lesssim 10^{-6}$ eV.

QCD axions are hypothetical particles introduced to solve the strong CP problem, namely the non-observation of CP violation from QCD interactions [1–4], see e.g., refs. [5,6] for recent reviews. They are pseudo-scalar Nambu-Goldstone bosons associated with the spontaneous breaking of the so-called Peccei-Quinn symmetry. Additionally, QCD axions are also a viable dark matter (DM) candidate, possibly accounting for the entirety of cold DM in the Universe. They can be produced through different thermal and non-thermal mechanisms in the early Universe, before or after inflation [7–9]. The allowed range of the Peccei-Quinn scale, f_a, to obtain the observed DM relic density is $10^{10} - 10^{12}$ GeV, corresponding to masses m_a in the rage $10^{-6} - 10^{-3}$ eV. The QCD DM axion stands as a key focus in the ongoing and future program of astroparticle physics investigations. Numerous experimental searches, both in the laboratory and in the sky have been designed to look for this particle [10–12].

Furthermore, several beyond-the-standard-model theories, such as string theory models [13], predict in many cases one or more axion-like particles (ALPs), with properties very similar to those of axions but not necessarily related to the strong CP-problem [14]. ALPs can have masses as low as 10^{-22} eV and are typically very weakly coupled to the SM. Moreover, they are also good DM candidates in some portions of the parameter space [15].

Experimental searches for both the QCD axion and ALPs often rely on their coupling to photons [16]. In both cases, the coupling is described by the effective Lagrangian term $\mathcal{L} \propto g_{a\gamma} a F_{\mu\nu} \tilde{F}^{\mu\nu}$.

One of the most promising ALP[1] searches with astrophysical probes involve the radio signal associated with ALP-photon conversion in magnetized astrophysical plasma. This signature is based on the above-mentioned ALP-photon coupling, and it would appear as a nearly monochromatic spectral line. In order to have a significant probability of conversion, large magnetic fields and dense plasma are required so to resonantly amplify the process. In the past few years, the search has been focused especially on the magnetosphere of neutron stars [17–34].

In this paper, we instead highlight that the Sun and its sunspots are promising targets. Sunspots are magnetic structures located within active regions of the Sun. They appear darker on the solar surface than the normal solar photosphere (quiet Sun) and are composed of an inner, darker part, called the umbra, and an outer, less dark part, called the penumbra. It is well known that the magnetic field can be very intense above the photosphere of sunspots, reaching a few thousand Gauss in the umbra [35]. The magnetic field decreases with height in the solar atmosphere, but it could still be rather strong in the chromosphere and corona. For example, Ref. [36] reported a magnetic field of about 4000 G at the base of the corona above a sunspot, with 1000 G at a height of 10^4 km. Sunspots might be environments hosting copious axion-photon conversions in their magnetic field.

The idea of considering the Sun was proposed in [37] for a similar process, i.e. investigating dark photon-photon mixing. A search for the associated monochromatic radio signal in the solar observation data of

the LOFAR telescope was then conducted in [38], which also discusses the application to the axion-photon conversion.

Besides non-relativistic DM axions, one could also consider the conversion of relativistic axions thermally produced in the Sun's interior and then converted into photons in the Sun's atmosphere [39]. In this case, they would lead to X-ray signatures, which we plan to investigate in a forthcoming analysis [40].

This paper aims to provide a simple and general description of the radio emission arising from the conversion of ambient DM axions in the Sun's magnetic field. The goal is to present robust and broad arguments with computations that can be easily reproduced by the reader. These arguments should provide a framework that can later be applied to specific examples in dedicated studies. As we shall see, the analysis of the radio signal from axion conversion in the solar magnetic field may provide an opportunity to access regions of unexplored parameter space with the next generation of radio telescopes.

For a non-relativistic axion, a weakly magnetized plasma, and assuming the magnetic field to be static, the conversion probability can be approximated as [32]

$$P_{a \to \gamma} \simeq \frac{\pi}{2} \frac{g_{a\gamma}^2 B_\perp^2}{v_a \omega'_{q|res}} , \tag{1}$$

where ω_q is the plasma frequency and $\omega'_{q|res}$ is its gradient $d\omega_q/dr$ evaluated at the resonance location, i.e., at the radius r_c where $\omega_q \simeq m_a$. In eq. (1) and in the following, we assume spherical symmetry and, for simplicity, radial emission. The radius r_c at which the conversion occurs, for different ALP masses, can be estimated from the resonance condition and the relation $\omega_q(r) = 1.17 \, \mu\text{eV} \sqrt{n_e(r)/(10^9 \, \text{cm}^{-3})}$, where n_e is the electron plasma density.

For a uniform conversion over a surface ΔA, and assuming the ALP distribution to be isotropic, the ALP-induced photons flux per unit frequency on Earth can be estimated as

$$S = \int \frac{d\Omega}{4\pi \, \Delta\nu} \rho_a v_a P_{a \to \gamma} e^{-\tau}$$
$$\simeq \frac{\Delta A}{4\pi \, \Delta\nu \, d^2} \rho_a v_a P_{a \to \gamma} e^{-\tau} , \tag{2}$$

where d is the distance of the conversion surface from us, ρ_a is the DM density at the conversion surface, τ is the photon optical depth, and $\Delta\nu$ is the bandwidth of the signal.

To gain some intuition about the expected signal, let us consider a sunspot, i.e., a structure with strong magnetic fields appearing on the solar surface. Considering a radius of the sunspot ℓ_s, the conversion area is computed as $\Delta A = \pi \ell_s^2$. For an analytical estimate, we can approximate the plasma profile as a power-law $\omega_p \propto h^\alpha$, with $\alpha \simeq 0.5$ in the range of conversion radii of interest. Then we have $\omega'_{q|res} = \alpha \omega_p/h_c$, where h_c is the distance of the conversion surface from the photosphere. Plugging in typical values for a large sunspot [35], we find

$$S = \frac{\Delta A}{8 \, \Delta\nu \, d^2} \rho_a \frac{g_{a\gamma}^2 B^2}{\omega'_{q|res}} e^{-\tau} = 0.7 \, \text{mJy} \left(\frac{10^{-6}}{\Delta\nu/\nu} \right)$$
$$\times \left(\frac{\ell_s}{4 \times 10^4 \, \text{km}} \right)^2 \left(\frac{\rho_a}{1.0 \, \text{GeV/cm}^3} \right) \left(\frac{g_{a\gamma}}{10^{-12} \, \text{GeV}^{-1}} \right)^2$$
$$\times \left(\frac{B_\perp}{10 \, \text{G}} \right)^2 \left(\frac{\mu\text{eV}}{m_a} \right)^2 \left(\frac{0.5}{\alpha} \right) \left(\frac{h_c}{3 \times 10^3 \, \text{km}} \right) e^{-\tau} . \tag{3}$$

In the previous equation, we have considered a local DM density $\rho_\infty = 0.3 \, \text{GeV cm}^{-3}$ far away from the Sun and accounted for the gravitational focusing of the Sun following [41]. This leads to a DM density at the solar surface of $\rho_a \simeq 1 \, \text{GeV cm}^{-3}$. Moreover, taking a local DM velocity dispersion $v \simeq 10^{-3}$ leads to a intrinsic bandwidth $\Delta\nu \simeq 10^{-6}$. In the following, in our numerical analysis performed to derive the sensitivity forecasts, the plasma frequency and its gradient are computed from the solar electron density distribution of Ref. [42]. We find that
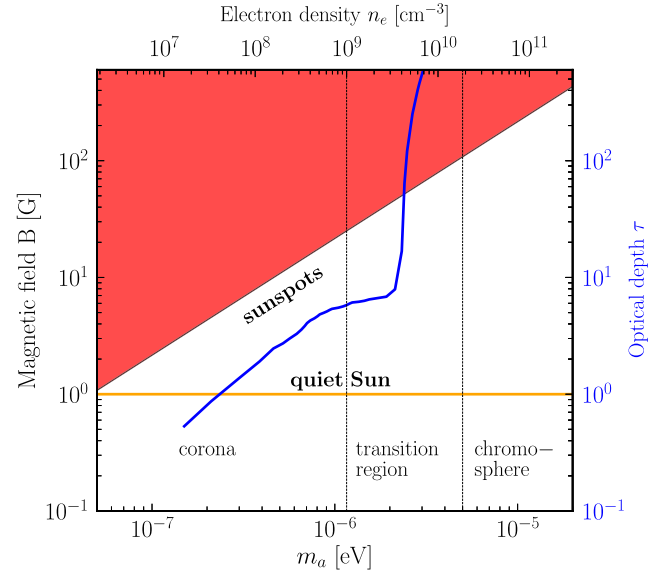
Fig. 1. In the red region, the electron cyclotron resonance causes a strong absorption of the photons produced by ALPs conversion during their propagation in the solar atmosphere. Assuming that the magnetic field decreases monotonically with distance from the photosphere, this effect does not occur when the magnetic field at the ALP conversion location lies in the white region. The optical depth associated with thermal bremsstrahlung, the other main absorption mechanism, is shown in blue (right-axis). The top axis shows the electron density at which the plasma frequency matches the ALP mass (bottom axis), and the resonant conversion can occur. Vertical lines mark different regions of the solar atmosphere. The orange horizontal line marks the typical value of 1 G of the magnetic field in the corona for the quiet Sun.

adopting a different model, e.g. [43], leads to a similar sensitivity on the axion signal.

Let us now analyze the absorption term. There are two main contributions to the opacity in the solar atmosphere at these wavelengths: the gyro-resonance absorption and the thermal bremsstrahlung. The first effect occurs when the resonant condition $m_a \simeq n \Omega_B(r)$ is met, where $\Omega_B = e \, B/m_e \simeq 0.012 \, \mu\text{eV} \, B/\text{G}$ is the electron cyclotron frequency and the integer n corresponds to the different energy levels. To compute the location where the cyclotron resonance is realized, we assume that the magnetic field decays with height following a power-law behavior after the ALP conversion point. Then, we extract the electron number density and the temperature of the plasma at the cyclotron resonance point. Finally, with these ingredients and following Ref. [44], we obtain the cyclotron optical depth. We find that for any reasonable choice of the magnetic field profile in the solar atmosphere, the optical depth τ_g is very large for the first three transitions $n = 1, 2, 3$, while $\tau_g \lesssim 1$ for $n = 4$ and negligible for higher levels. Therefore, assuming a monotonically decreasing magnetic field and plasma density, we conservatively assume that photons from axion conversion can reach the Earth only if the conversion happens after the surface of gyro-resonance absorption associated with the $n = 4$ level. This condition translates into an upper limit of the magnetic field at the ALP conversion point, which is represented in Fig. 1, with the *no-signal region* shown in red.

Concerning the thermal bremsstrahlung, the absorption coefficient reads [45]:

$$\alpha_b \simeq 0.018 \, \frac{n_e}{10^6 \, \text{cm}^{-3}} \frac{Z_{eff}^2 n_i}{10^6 \, \text{cm}^{-3}} \left(\frac{T}{\text{K}} \right)^{-3/2} \left(\frac{\nu}{\text{MHz}} \right)^{-2} G_F , \tag{4}$$

where n_i is the number density of ions with effective charge Z_{eff}, T is the temperature of the plasma, all taken from [42], and G_F is the Gaunt factor, for which we referred to [46]. In the corona, the plasma is essentially fully ionized, and $Z_{eff} \approx 1$, while this is not the case in the chromosphere and transition region. The bremsstrahlung optical depth

$\tau_b = \int_{h_c} d\ell \, \alpha_b$ is shown as a blue line in Fig. 1. In the chromosphere, we have $\tau_b \gg 1$ therefore the ALP signal is completely absorbed. On the other hand, in the corona $\tau_b \lesssim \mathcal{O}(1)$.

A crucial ingredient is the magnetic field in the corona, which determines the conversion probability as described in eq. (1). The magnetic field of the quiet Sun has a strength between $1 - 4$ G, on average [47]. We will take $B = 1$ G when estimating the ALP signal from across the whole Sun. As mentioned before, the magnetic field of sunspots can be very intense, even above the photosphere. Sunspot observations accumulated over the years show great variability of their properties, with sizes ranging from 10 to 10^5 km, and magnetic fields from few G up to few thousand G [35].

Here, in the spirit of providing a general treatment, we will assume sunspots to populate the white triangle in Fig. 1, delimited by the red region and orange line. Namely, we assume that there exist sunspots with associated magnetic fields in the corona and transition region, where the resonance ALP conversion occurs, larger than the magnetic field of the quiet Sun, and up to the maximal value allowed by the cyclotron absorption, see Fig. 1. For the sake of concreteness, in the following, we will consider two cases: one where the magnetic field maximizes the signal, i.e. lies at the border between the red and white regions in Fig. 1, and one where we simply assume $B = 4$ G at the ALP conversion radius above the sunspot.

To examine observational prospects, we derive forecasts for the first phase of the SKA observatory, which is expected to be completed in its final configuration in 2029. We follow [48], in particular their Table 6 provides the line sensitivity for sources with an angular size within a certain range. For larger extensions, we assume a linear degradation of the sensitivity with the angular size of the source, as suggested by their Table 4 for our range of interest.

The angular radius of a sunspot is typically smaller than a few arcmin, e.g. $\ell_s = 4 \times 10^4$ km, which we will use for our estimates, corresponds to $0.9'$. On the other hand, radio photons are affected by scattering processes during their propagation in the solar plasma, which leads to an angular smearing of the signal. We estimate the broadening of a point-like source as described in [49]. In the case of the entire Sun, this broadening is instead marginal. The same conclusion has also been reported in [50], finding that the observed radio size of the Sun at 100-240 MHz is only 25–30% larger in area than the intrinsic one.

Finally, the line sensitivity reported in [48] refers to observations of regions of the sky without strong radio emissions. Therefore, to include the large radio background produced by the Sun, we correct the quoted sensitivity adding the flux density of the Sun to the system-equivalent flux density of an SKA station. Concretely, we follow the estimates provided in [51]. From Fig. 8 in [48], we can read the sensitivity of the SKA-Low array in terms of A_{eff}/T_{sys} and convert it into the System Equivalent Flux Density $SEFD = 2k_B T_{sys}/A_{eff}$. Since the array is composed by 512 stations, the $SEFD_s$ of an SKA station (which sees the Sun as a point-like source) is about 512 times the $SEFD$ of the SKA array. To derive the sensitivity, the measured $SEFD_S$ including any emission along the direction of observation has to be added. In this case the Sun gives the dominant contribution, and the degradation of the sensitivity with respect to a region with low radio emission is given by the factor $(SEFD_s + SEFD_S)/SEFD_s$.

Following the procedure explained above, we obtain the results presented in Fig. 2. The projected sensitivity is at 95% C.L., namely, they correspond to couplings providing a conversion signal equal to twice the SKA sensitivity. For ALP masses in the range $10^{-6} - 10^{-7}$ eV, the proposed search strategy can improve existing laboratory bounds, and it is competitive with existing astrophysical constraints. We find that the forecasted sensitivities for observations of the entire Sun and a sunspot with a large magnetic field are comparable. A technical advantage in the latter case is offered by the small angular size of the emission region, in contrast to the case of the entire Sun, where the large angular extension requires care in the data manipulation. On the other hand, the properties of a sunspot needed to compute the prediction of the
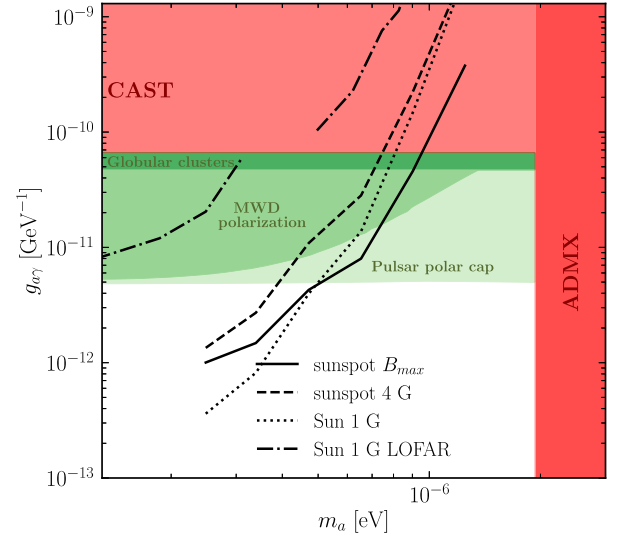
Fig. 2. Projected sensitivity on the ALP-photon coupling $g_{a\gamma}$ versus ALP mass m_a, assuming 100 hours of observations with SKA-1 Low, of a sunspot having the maximum magnetic field allowed by the gyro-resonance absorption condition at the conversion location (see Fig. 1) (solid), a sunspot with a magnetic field of 4 G at the conversion location (dashed), and the whole Sun (dotted). The radius of the conversion surface above a sunspot is taken to be $\ell_s = 4 \times 10^4$ km. The dashed-dotted line shows the projected sensitivity for the whole Sun, in the case of a 8hr-observation with LoFAR [52]. In red, we show the laboratory bounds from ADMX [53] and CAST [54], while in green we show astrophysical bounds: the R2-parameter in globular cluster [55], and the most conservative limits from polarization of magnetic dwarf [56] and ALP production in pulsar polar caps [57]. Other relevant constraints in this mass range (not shown in the figure for clarity) come from the R-parameter in globular clusters [58], X-ray observations of magnetic white dwarfs [59] and from γ-ray observation of the blazar Markarian 421 (Mrk 421) [60,61].

expected flux might not be straightforward to be derived from the observations.

The curves in Fig. 2 are computed assuming an observing time of $\Delta t = 100$ hr. Considering that solar physics is one of the key scientific goals of the SKAO [62], hundreds of hours of observations of the Sun are foreseen. In the case of sunspots, the 100 hr value is guaranteed if intended as a combination of different sunspots, whilst it is probably difficult to achieve for a single one. Note that, in any case, the sensitivity to the ALP-photon coupling scales very moderately with observing time, as $\Delta t^{1/4}$.

In Fig. 2, we assume a bandwidth of $\Delta\nu/\nu = 10^{-6}$, matching the one induced by the dispersion of the DM velocity. This is achievable by the SKA Low. On the other hand, this value might be somewhat optimistic since it neglects possible smearing effects.[2] Note, however, that, again, the sensitivities scale as $(\Delta\nu/\nu)^{1/4}$, so even significantly larger bandwidths can still lead to interesting prospects.

Let us also mention that the proposed SKAO observation requires a high level of dynamic range, being 4×10^5 at the smallest frequency/mass up to 3×10^6 at the highest frequency/mass. A dynamic range of the order of 10^6 is challenging, and it certainly requires significant care and effort in the data calibration and analysis. However, it is in the range of values reported in the literature [63], and such a spectral dynamic range is of the same order required for observations of the 21 cm line from the epoch of reionization, which have made steady progress towards achieving it [64,65].

---

[2] We postpone a full ray-tracing computation to simulate photon propagation in the Sun to future work. Here, we accounted for absorption and spatial broadening as described in the text. The bandwidth smearing is instead neglected for simplicity.

For completeness, we report the sensitivity that can be obtained with current instruments. We focus on the LoFAR telescope [52] and derive prospects for a typical observation, i.e., the 24-station array, 8 hours of integration time and 100 kHz/channel of frequency resolution (an analysis with available data and weaker sensitivity is described in [38]). The forecast computation proceeds as discussed above for the SKAO. We can see from Fig. 2 that the projected sensitivity falls in a strongly constrained region of the parameter space. The higher sensitivity of the SKAO and/or a dedicated campaign seem to be required to test viable models.

Let us notice that other bounds derived from radio observations, e.g., the one from [57], can also be improved by SKAO observations, possibly surpassing the projected sensitivity described here. However, they rely on different assumptions, and the Sun can be seen as a complementary probe.

To conclude, in this work, we highlighted that the Sun can be a promising target for looking for radio waves from ALP conversion. A discussion in this direction was recently reported also in [38]. Here we presented a simple and general derivation of the expected signal, with forecasts for the SKA, and added the case of sunspots. The Sun can be thus considered as complementary/alternative to the case of neutron stars, which are the target that has been extensively investigated in connection to the ALP conversion [17–34]. As a simple comparison let us consider the case of a nearby isolated neutron star, keeping in mind however that neutron stars could also be located in environments hosting DM densities much larger than the local one, such as the galactic center. Focusing on the main ingredients determining the radio flux, we have

$$
\begin{aligned}
S &\propto \left(\frac{h_{c,s}\, \ell_s^2}{5 \times 10^{12}\, \mathrm{km}^3} \right) \left(\frac{B_s}{5\, \mathrm{G}} \right)^2 \left(\frac{1.5 \times 10^8\, \mathrm{km}}{d_s} \right)^2 \\
&\simeq \left(\frac{r_{c,NS}}{200\, \mathrm{km}} \right)^3 \left(\frac{B_{NS}}{10^{12}\, \mathrm{G}} \right)^2 \left(\frac{1\, \mathrm{kpc}}{d_{NS}} \right)^2 ,
\end{aligned}
\tag{5}
$$

where s denotes a large sunspot and NS a neutron star. Therefore, naively, we see that the expected signals are roughly comparable in order of magnitude. However, there are important differences between the two systems, in terms of systematic uncertainties and values of the relevant parameters. Hence, the two approaches present complementary ways to explore the parameter space corresponding to ALP dark matter. Since the properties of the Sun are much better known and certainly more easily accessible to future measurements, what is presented here could be a more robust and accessible method to probe the ALP parameter space in the sub μeV region. Unfortunately, absorption effects limit the range of masses that can be probed to $m_a \lesssim 10^{-6}$ eV, as discussed in the text. This also implies that low-frequency radio observations will be the key to test the hypothesis discussed here.

Declaration of competing interest

The authors declare the following financial interests/personal relationships which may be considered as potential competing interests: Elisa Todarello reports financial support was provided by University of Turin. If there are other authors, they declare that they have no known competing financial interests or personal relationships that could have appeared to influence the work reported in this paper.

Data availability

No data was used for the research described in the article.

Acknowledgements

References

[1] R.D. Peccei, H.R. Quinn, CP conservation in the presence of instantons, Phys. Rev. Lett. 38 (1977) 1440 [328 (1977)].

[2] R.D. Peccei, H.R. Quinn, Constraints imposed by CP conservation in the presence of instantons, Phys. Rev. D 16 (1977) 1791.

[3] S. Weinberg, A new light boson?, Phys. Rev. Lett. 40 (1978) 223.

[4] F. Wilczek, Problem of strong p and t invariance in the presence of instantons, Phys. Rev. Lett. 40 (1978) 279.

[5] J.E. Kim, G. Carosi, Axions and the strong CP problem, Rev. Mod. Phys. 82 (2010) 557, Erratum: Rev. Mod. Phys. 91 (2019) 049902, arXiv:0807.3125 [hep-ph].

[6] L. Di Luzio, M. Giannotti, E. Nardi, L. Visinelli, The landscape of QCD axion models, Phys. Rep. 870 (2020) 1, arXiv:2003.01100 [hep-ph].

[7] J. Preskill, M.B. Wise, F. Wilczek, Cosmology of the invisible axion, Phys. Lett. B 120 (1983) 127 [URL (1982)].

[8] L.F. Abbott, P. Sikivie, A cosmological bound on the invisible axion, Phys. Lett. B 120 (1983) 133 [URL (1982)].

[9] M. Dine, W. Fischler, The not so harmless axion, Phys. Lett. B 120 (1983) 137 [URL (1982)].

[10] A.S. Chou, et al., Snowmass cosmic frontier report, in Snowmass 2021, arXiv:2211.09978 [hep-ex], 2022.

[11] C.B. Adams, et al., Axion dark matter, in Snowmass 2021, arXiv:2203.14923 [hep-ex], 2022.

[12] C. Antel, et al., Feebly interacting particles: FIPs 2022 workshop report, in workshop on feebly-interacting particles, arXiv:2305.01715 [hep-ph], 2023.

[13] A. Arvanitaki, S. Dimopoulos, N. Dubovsky, N. Kaloper, J. March-Russell, String Axiverse, Phys. Rev. D 81 (2010) 123530, arXiv:0905.4720 [hep-th].

[14] J. Jaeckel, A. Ringwald, The low-energy frontier of particle physics, Annu. Rev. Nucl. Part. Sci. 60 (2010) 405, arXiv:1002.0329 [hep-ph].

[15] P. Arias, D. Cadamuro, M. Goodsell, J. Jaeckel, J. Redondo, A. Ringwald, WISPy cold dark matter, J. Cosmol. Astropart. Phys. 06 (2012) 013, arXiv:1201.5902 [hep-ph].

[16] P. Sikivie, Experimental tests of the invisible axion, particle physics and cosmology: dark matter, Phys. Rev. Lett. 51 (1983) 1415 [321 (1983)].

[17] M.S. Pshirkov, S.B. Popov, Conversion of dark matter axions to photons in magnetospheres of neutron stars, J. Exp. Theor. Phys. 108 (2009) 384, arXiv:0711.1264 [astro-ph].

[18] A. Hook, Y. Kahn, B.R. Safdi, Z. Sun, Radio signals from axion dark matter conversion in neutron star magnetospheres, Phys. Rev. Lett. 121 (2018) 241102, arXiv:1804.03145 [hep-ph].

[19] B.R. Safdi, Z. Sun, A.Y. Chen, Detecting axion dark matter with radio lines from neutron star populations, Phys. Rev. D 99 (2019) 123021, arXiv:1811.01020 [astro-ph.CO].

[20] F.P. Huang, K. Kadota, T. Sekiguchi, H. Tashiro, Radio telescope search for the resonant conversion of cold dark matter axions from the magnetized astrophysical sources, Phys. Rev. D 97 (2018) 123001, arXiv:1803.08230 [hep-ph].

[21] R.A. Battye, B. Garbrecht, J.I. McDonald, F. Pace, S. Srinivasan, Dark matter axion detection in the radio/mm-waveband, Phys. Rev. D 102 (2020) 023504, arXiv:1910.11907 [astro-ph.CO].

[22] M. Leroy, M. Chianese, T.D.P. Edwards, C. Weniger, Radio signal of axion-photon conversion in neutron stars: a ray tracing analysis, Phys. Rev. D 101 (2020) 123003, arXiv:1912.08815 [hep-ph].

[23] J.W. Foster, Y. Kahn, O. Macias, Z. Sun, R.P. Eatough, V.I. Kondratiev, W.M. Peters, C. Weniger, B.R. Safdi, Green bank and Effelsberg radio telescope searches for axion dark matter conversion in neutron star magnetospheres, Phys. Rev. Lett. 125 (2020) 171301, arXiv:2004.00011 [astro-ph.CO].

[24] A. Prabhu, N.M. Rapidis, Resonant conversion of dark matter oscillons in pulsar magnetospheres, J. Cosmol. Astropart. Phys. 10 (2020) 054, arXiv:2005.03700 [astro-ph.CO].

[25] S.J. Witte, D. Noordhuis, T.D.P. Edwards, C. Weniger, Axion-photon conversion in neutron star magnetospheres: the role of the plasma in the Goldreich-Julian model, Phys. Rev. D 104 (2021) 103030, arXiv:2104.07670 [hep-ph].

[26] R.A. Battye, B. Garbrecht, J.I. McDonald, S. Srinivasan, Radio line properties of axion dark matter conversion in neutron stars, J. High Energy Phys. 09 (2021) 105, arXiv:2104.08290 [hep-ph].

[27] R.A. Battye, J. Darling, J.I. McDonald, S. Srinivasan, Towards robust constraints on axion dark matter using PSR J1745-2900, Phys. Rev. D 105 (2022) L021305, arXiv:2107.01225 [astro-ph.CO].

[28] J.-W. Wang, X.-J. Bi, P.-F. Yin, Detecting axion dark matter through the radio signal from Omega Centauri, Phys. Rev. D 104 (2021) 103015, arXiv:2109.00877 [astro-ph.HE].

[29] J.W. Foster, S.J. Witte, M. Lawson, T. Linden, V. Gajjar, C. Weniger, B.R. Safdi, Extraterrestrial axion search with the breakthrough listen galactic center survey, Phys. Rev. Lett. 129 (2022) 251102, arXiv:2202.08274 [astro-ph.CO].

[30] Y.-F. Zhou, et al., Searching for axion dark matter with the MeerKAT radio telescope, Phys. Rev. D 106 (2022) 083006, arXiv:2209.09695 [astro-ph.CO].

[31] J.I. McDonald, S.J. Witte, Generalized ray tracing for axions in astrophysical plasmas, Phys. Rev. D 108 (2023) 103021, arXiv:2309.08655 [hep-ph].

[32] J.I. McDonald, B. Garbrecht, P. Millington, Axion-photon conversion in 3D media and astrophysical plasmas, J. Cosmol. Astropart. 12 (2023) 031, arXiv:2307.11812 [hep-ph].

[33] J. Tjemsland, J. McDonald, S.J. Witte, Adiabatic axion-photon mixing near neutron stars, arXiv:2310.18403 [hep-ph], 2023.

[34] J.H. Buckley, P.B. Dev, F. Ferrer, F.P. Huang, Fast radio bursts from axion stars moving through pulsar magnetospheres, Phys. Rev. D 103 (2021), https://doi.org/10.1103/physrevd.103.043015.

[35] S.K. Solanki, Sunspots: an overview, Astron. Astrophys. Rev. 11 (2003) 153.

[36] S.A. Anfinogentov, A.G. Stupishin, I.I. Mysh'yakov, G.D. Fleishman, Record-breaking coronal magnetic field in solar active region 12673, Astrophys. J. Lett. 880 (2019) L29, arXiv:1907.06398 [astro-ph.SR].

[37] H. An, F.P. Huang, J. Liu, W. Xue, Radio-frequency dark photon dark matter across the sun, Phys. Rev. Lett. 126 (2021) 181102, arXiv:2010.15836 [hep-ph].

[38] H. An, X. Chen, S. Ge, J. Liu, Y. Luo, Searching for ultralight dark matter conversion in solar corona using low frequency array data, Nat. Commun. 15 (2024) 915, arXiv:2301.03622 [hep-ph].

[39] E.D. Carlson, L.-S. Tseng, Pseudoscalar conversion and x-rays from the sun, Phys. Lett. B 365 (1996) 193, arXiv:hep-ph/9507345.

[40] E. Todarello, et al., in preparation.

[41] M.S. Alenazi, P. Gondolo, Phase-space distribution of unbound dark matter near the Sun, Phys. Rev. D 74 (2006) 083518, arXiv:astro-ph/0608390.

[42] C.L. Selhorst, A.V.R. Silva, J.E.R. Costa, Solar atmospheric model with spicules applied to radio observation, Astron. Astrophys. 433 (2005) 365.

[43] V. De La Luz, A. Lara, E. Mendoza, M. Shimojo, 3D simulations of the quiet sun radio emission at millimeter and submillimeter wavelengths, Geofís. Int. 47 (2008) 197.

[44] G.A. Dulk, Radio emission from the sun and stars, Annu. Rev. Astron. Astrophys. 23 (1985) 169.

[45] G.B. Rybicki, A.P. Lightman, Radiative Processes in Astrophysics, 1986.

[46] J. Chluba, A. Ravenni, B. Bolliet, Improved calculations of electron-ion bremsstrahlung Gaunt factors for astrophysical applications, Mon. Not. R. Astron. Soc. 492 (2020) 177, arXiv:1911.08861 [astro-ph.CO].

[47] Z. Yang, C. Bethge, H. Tian, S. Tomczyk, R. Morton, G. Del Zanna, S.W. McIntosh, B.B. Karak, S. Gibson, T. Samanta, J. He, Y. Chen, L. Wang, Global maps of the magnetic field in the solar corona, Science 369 (2020) 694, arXiv:2008.03136 [astro-ph.SR].

[48] R. Braun, A. Bonaldi, T. Bourke, E. Keane, J. Wagg, Anticipated performance of the square kilometre array – phase 1, arXiv e-prints, arXiv:1912.12699 [astro-ph.IM], 2019.

[49] E.P. Kontar, X. Chen, N. Chrysaphi, N.L.S. Jeffrey, A.G. Emslie, V. Krupar, M. Maksimovic, M. Gordovskyy, P.K. Browning, Anisotropic radio-wave scattering and the interpretation of solar radio emission observations, Astrophys. J. 884 (2019) 122, arXiv:1909.00340 [astro-ph.SR].

[50] R. Sharma, D. Oberoi, Propagation effects in quiet sun observations at meter wavelengths, Astrophys. J. 903 (2020) 126, arXiv:2009.10604 [astro-ph.SR].

[51] G. Macario, G. Pupillo, G. Bernardi, P. Bolli, P. Di Ninni, G. Comoretto, A. Mattana, J. Monari, F. Perini, M. Schiaffino, M. Sokolowski, R. Wayth, J. Broderick, M. Waterson, M. Grazia Labate, R. Chiello, A. Magro, T. Booler, A. Mcphail, D. Minchin, R. Bhushan, Characterization of the SKA1-low prototype station aperture array verification system 2, J. Astron. Telesc. Instrum. Syst. 8 (2022) 011014, arXiv:2109.11983 [astro-ph.IM].

[52] M.P. van Haarlem, M.W. Wise, A.W. Gunst, G. Heald, J.P. McKean, J.W.T. Hessels, A.G. de Bruyn, R. Nijboer, J. Swinbank, R. Fallows, M. Brentjens, A. Nelles, R. Beck, H. Falcke, R. Fender, J. Hörandel, L.V.E. Koopmans, G. Mann, G. Miley, H. Röttgering, B.W. Stappers, R.A.M.J. Wijers, S. Zaroubi, M. van den Akker, A. Alexov, J. Anderson, K. Anderson, A. van Ardenne, M. Arts, A. Asgekar, I.M. Avruch, F. Batejat, L. Bähren, M.E. Bell, M.R. Bell, I. van Bemmel, P. Bennema, M.J. Bentum, G. Bernardi, P. Best, L. Bîrzan, A. Bonafede, A.J. Boonstra, R. Braun, J. Bregman, F. Breitling, R.H. van de Brink, J. Broderick, P.C. Broekema, W.N. Brouw, M. Brüggen, H.R. Butcher, W. van Cappellen, B. Ciardi, T. Coenen, J. Conway, A. Coolen, A. Corstanje, S. Damstra, O. Davies, A.T. Deller, R.J. Dettmar, G. van Diepen, K. Dijkstra, P. Donker, A. Doorduin, J. Dromer, M. Drost, A. van Duin, J. Eislöffel, J. van Enst, C. Ferrari, W. Frieswijk, H. Gankema, M.A. Garrett, F. de Gasperin, M. Gerbers, E. de Geus, J.M. Grießmeier, T. Grit, P. Gruppen, J.P. Hamaker, T. Hassall, M. Hoeft, H.A. Holties, A. Horneffer, A. van der Horst, A. van Houwelingen, A. Huijgen, M. Iacobelli, H. Intema, N. Jackson, V. Jelic, A. de Jong, E. Juette, D. Kant, A. Karastergiou, A. Koers, H. Kollen, V.I. Kondratiev, E. Kooistra, Y. Koopman, A. Koster, M. Kuniyoshi, M. Kramer, G. Kuper, P. Lambropoulos, C. Law, J. van Leeuwen, J. Lemaitre, M. Loose, P. Maat, G. Macario, S. Markoff, J. Masters, R.A. McFadden, D. McKay-Bukowski, H. Meijering, H. Meulman, M. Mevius, E. Middelberg, R. Millenaar, J.C.A. Miller-Jones, R.N. Mohan, J.D. Mol, J. Morawietz, R. Morganti, D.D. Mulcahy, E. Mulder, H. Munk, L. Nieuwenhuis, R. van Nieuwpoort, J.E. Noordam, M. Norden, A. Noutsos, A.R. Offringa, H. Olofsson, A. Omar, E. Orrú, R. Overeem, H. Paas, M. Pandey-Pommier, V.N. Pandey, R. Pizzo, A. Polatidis, D. Rafferty, S. Rawlings, W. Reich, J.P. de Reijer, J. Reitsma, G.A. Renting, P. Riemers, E. Rol, J.W. Romein, J. Roosjen, M. Ruiter, A. Scaife, K. van der Schaaf, B. Scheers, P. Schellart, A. Schoenmakers, G. Schoonderbeek, M. Serylak, A. Shulevski, J. Sluman, O. Smirnov, C. Sobey, H. Spreeuw, M. Steinmetz, C.G.M. Sterks, H.J. Stiepel, K. Stuurwold, M. Tagger, Y. Tang, C. Tasse, I. Thomas, S. Thoudam, M.C. Toribio, B. van der Tol, O. Usov, M. van Veelen, A.J. van der Veen, S. ter Veen, J.P.W. Verbiest, R. Vermeulen, N. Vermaas, C. Vocks, C. Vogt, M. de Vos, E. van der Wal, R. van Weeren, H. Weggemans, P. Weltevrede, S. White, S.J. Wijnholds, T. Wilhelmsson, O. Wucknitz, S. Yatawatta, P. Zarka, A. Zensus, J. van Zwieten, LOFAR: the LOw-Frequency ARray, Astron. Astrophys. 556 (2013) A2, arXiv:1305.3550 [astro-ph.IM].

[53] S.J. Asztalos, G. Carosi, C. Hagmann, D. Kinion, K. van Bibber, M. Hotz, L.J. Rosenberg, G. Rybka, J. Hoskins, J. Hwang, P. Sikivie, D.B. Tanner, R. Bradley, J. Clarke, Squid-based microwave cavity search for dark-matter axions, Phys. Rev. Lett. 104 (2010), https://doi.org/10.1103/physrevlett.104.041301.

[54] New Cast Limit on the Axion–Photon Interaction, Nat. Phys. 13 (2017) 584–590.

[55] M.J. Dolan, F.J. Hiskens, R.R. Volkas, Advancing globular cluster constraints on the axion-photon coupling, J. Cosmol. Astropart. 2022 (10) (2022) 096.

[56] C. Dessert, D. Dunsky, B.R. Safdi, Upper limit on the axion-photon coupling from magnetic white dwarf polarization, Phys. Rev. D 105 (2022), https://doi.org/10.1103/physrevd.105.103034.

[57] D. Noordhuis, A. Prabhu, S.J. Witte, A.Y. Chen, F. Cruz, C. Weniger, Novel constraints on axions produced in pulsar polar-cap cascades, arXiv:2209.09917 [hep-ph], 2023.

[58] A. Ayala, I. Domínguez, M. Giannotti, A. Mirizzi, O. Straniero, Revisiting the bound on axion-photon coupling from globular clusters, Phys. Rev. Lett. 113 (2014), https://doi.org/10.1103/physrevlett.113.191302.

[59] C. Dessert, A.J. Long, B.R. Safdi, No evidence for axions from Chandra observation of the magnetic white dwarf re j0317-853, Phys. Rev. Lett. 128 (2022), https://doi.org/10.1103/physrevlett.128.071102.

[60] H.-J. Li, J.-G. Guo, X.-J. Bi, S.-J. Lin, P.-F. Yin, Limits on axionlike particles from mrk 421 with 4.5-year period observations by argo-ybj and Fermi-lat, Phys. Rev. D 103 (2021), https://doi.org/10.1103/physrevd.103.083003.

[61] H.-J. Li, X.-J. Bi, P.-F. Yin, Searching for axion-like particles with the blazar observations of magic and Fermi-lat *, Chin. Phys. C 46 (2022) 085105.

[62] A. Nindos, E.P. Kontar, D. Oberoi, Solar physics with the square kilometre array, Adv. Space Res. 63 (2019) 1404, arXiv:1810.04951 [astro-ph.SR].

[63] O.M. Smirnov, Revisiting the radio interferometer measurement equation. III. Addressing direction-dependent effects in 21 cm WSRT observations of 3C 147, Astron. Astrophys. 527 (2011) A108, arXiv:1101.1768 [astro-ph.IM].

[64] N. Barry, G. Bernardi, B. Greig, N. Kern, F. Mertens, SKA-low intensity mapping pathfinder updates: deeper 21 cm power spectrum limits from improved analysis frameworks, J. Astron. Telesc. Instrum. Syst. 8 (2021) 011007, arXiv:2110.06173 [astro-ph.CO].

[65] Z. Abdurashidova, et al., HERA, HERA phase I limits on the cosmic 21 cm signal: constraints on astrophysics and cosmology during the epoch of reionization, Astrophys. J. 924 (2022) 51, arXiv:2108.07282 [astro-ph.CO].